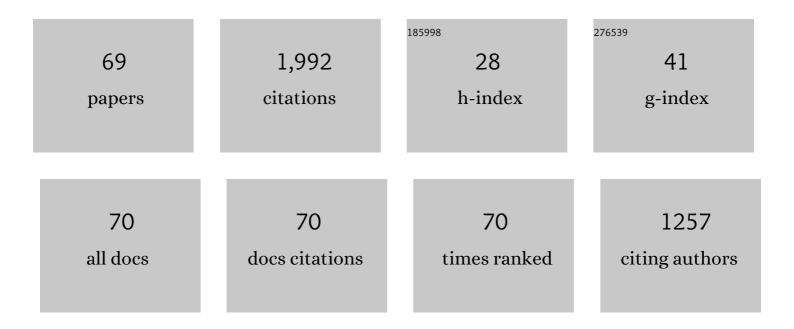
List of Publications by Year in descending order

Source: https://exaly.com/author-pdf/32089/publications.pdf Version: 2024-02-01



WENDINGLI

#	Article	IF	CITATIONS
1	GIS-based assessment of landslide susceptibility using certainty factor and index of entropy models for the Qianyang County of Baoji city, China. Journal of Earth System Science, 2015, 124, 1399-1415.	0.6	106
2	Effects of Coal Mining on Shallow Water Resources in Semiarid Regions: A Case Study in the Shennan Mining Area, Shaanxi, China. Mine Water and the Environment, 2017, 36, 104-113.	0.9	90
3	GIS-based landslide susceptibility mapping using analytical hierarchy process (AHP) and certainty factor (CF) models for the Baozhong region of Baoji City, China. Environmental Earth Sciences, 2016, 75, 1.	1.3	84
4	Landslide susceptibility mapping based on GIS and information value model for the Chencang District of Baoji, China. Arabian Journal of Geosciences, 2014, 7, 4499-4511.	0.6	76
5	Classification of the type of eco-geological environment of a coal mine district: A case study of an ecologically fragile region in Western China. Journal of Cleaner Production, 2018, 174, 1513-1526.	4.6	73
6	Effect of natural conditions and mining activities on vegetation variations in arid and semiarid mining regions. Ecological Indicators, 2019, 103, 331-345.	2.6	70
7	Landslide susceptibility assessment using frequency ratio, statistical index and certainty factor models for the Gangu County, China. Arabian Journal of Geosciences, 2016, 9, 1.	0.6	69
8	Predictive modeling of landslide hazards in Wen County, northwestern China based on information value, weights-of-evidence, and certainty factor. Geomatics, Natural Hazards and Risk, 2019, 10, 820-835.	2.0	69
9	Height of the Water-Flowing Fractured Zone of the Jurassic Coal Seam in Northwestern China. Mine Water and the Environment, 2018, 37, 312-321.	0.9	66
10	A GIS-based comparative evaluation of analytical hierarchy process and frequency ratio models for landslide susceptibility mapping. Physical Geography, 2017, 38, 318-337.	0.6	64
11	Application of analytic hierarchy process model for landslide susceptibility mapping in the Gangu County, Gansu Province, China. Environmental Earth Sciences, 2016, 75, 1.	1.3	56
12	Goaf water storage and utilization in arid regions of northwest China: A case study of Shennan coal mine district. Journal of Cleaner Production, 2018, 202, 33-44.	4.6	51
13	Application of Brillouin optical time domain reflectometry to dynamic monitoring of overburden deformation and failure caused by underground mining. International Journal of Rock Mechanics and Minings Sciences, 2018, 106, 133-143.	2.6	50
14	Application of frequency ratio, statistical index, and index of entropy models and their comparison in landslide susceptibility mapping for the Baozhong Region of Baoji, China. Arabian Journal of Geosciences, 2015, 8, 1829-1841.	0.6	46
15	Assessment of eco-geo-environment quality using multivariate data: A case study in a coal mining area of Western China. Ecological Indicators, 2019, 107, 105651.	2.6	44
16	Application of statistical index and index of entropy methods to landslide susceptibility assessment in Gongliu (Xinjiang, China). Environmental Earth Sciences, 2016, 75, 1.	1.3	43
17	An Improved Vulnerability Assessment Model for Floor Water Bursting from a Confined Aquifer Based on the Water Inrush Coefficient Method. Mine Water and the Environment, 2018, 37, 196-204.	0.9	43
18	Formation mechanism and prediction method of water inrush from separated layers within coal seam mining: A case study in the Shilawusu mining area, China. Engineering Failure Analysis, 2019, 103, 158-172.	1.8	42

#	Article	IF	CITATIONS
19	Zoning method for environmental engineering geological patterns in underground coal mining areas. Science of the Total Environment, 2018, 634, 1064-1076.	3.9	39
20	Evaluation of water inrush risk from coal seam floors with an AHP–EWM algorithm and GIS. Environmental Earth Sciences, 2019, 78, 1.	1.3	39
21	GIS-based landslide susceptibility analysis using frequency ratio and evidential belief function models. Environmental Earth Sciences, 2016, 75, 1.	1.3	36
22	Indicators sensitivity analysis for environmental engineering geological patterns caused by underground coal mining with integrating variable weight theory and improved matter-element extension model. Science of the Total Environment, 2019, 686, 606-618.	3.9	36
23	A comparative study on the landslide susceptibility mapping using logistic regression and statistical index models. Arabian Journal of Geosciences, 2017, 10, 1.	0.6	33
24	Risk Evaluation of Bed-Separation Water Inrush: A Case Study in the Yangliu Coal Mine, China. Mine Water and the Environment, 2018, 37, 288-299.	0.9	33
25	Characteristic of water chemistry and hydrodynamics of deep karst and its influence on deep coal mining. Arabian Journal of Geosciences, 2014, 7, 1261-1275.	0.6	32
26	Zoning and management of phreatic water resource conservation impacted by underground coal mining: A case study in arid and semiarid areas. Journal of Cleaner Production, 2019, 224, 677-685.	4.6	32
27	Effects of coal mining on the evolution of groundwater hydrogeochemistry. Hydrogeology Journal, 2019, 27, 2245-2262.	0.9	32
28	GIS based frequency ratio and index of entropy models to landslide susceptibility mapping (Daguan,) Tj ETQq0 0	0 rgBT /O 1.3	verlock 10 Tf
29	Water Inrush Risk zoning and Water Conservation Mining Technology in the Shennan Mining Area, Shaanxi, China. Arabian Journal for Science and Engineering, 2018, 43, 321-333.	1.7	31
30	Quantitative analysis of the relationship between vegetation and groundwater buried depth: A case study of a coal mine district in Western China. Ecological Indicators, 2019, 102, 770-782.	2.6	31
31	A comparative study on the landslide susceptibility mapping using evidential belief function and weights of evidence models. Journal of Earth System Science, 2016, 125, 645-662.	0.6	30
32	Numerical simulation for groundwater distribution after mining in Zhuanlongwan mining area based on visual MODFLOW. Environmental Earth Sciences, 2018, 77, 1.	1.3	28
33	Zoning method for mining-induced environmental engineering geological patterns considering the degree of influence of mining activities on phreatic aquifer. Journal of Hydrology, 2019, 578, 124020.	2.3	27
34	Landslide susceptibility mapping at Gongliu county, China using artificial neural network and weight of evidence models. Geosciences Journal, 2016, 20, 705-718.	0.6	25
35	Risk assessment of water inrush from aquifers underlying the Qiuji coal mine in China. Arabian Journal of Geosciences, 2019, 12, 1.	0.6	23
36	Study on failure depth of coal seam floor in deep mining. Environmental Earth Sciences, 2019, 78, 1.	1.3	22

#	Article	IF	CITATIONS
37	Investigation on mining-induced fractured zone height developed in different layers above Jurassic coal seam in western China. Arabian Journal of Geosciences, 2018, 11, 1.	0.6	19
38	Study on the Height of the Mining-Induced Water-Conducting Fracture Zone Under the Q2l Loess Cover of the Jurassic Coal Seam in Northern Shaanxi, China. Mine Water and the Environment, 2020, 39, 57-67.	0.9	18
39	Temporal and spatial evolution characteristics of fracture distribution of floor strata in deep coal seam mining. Engineering Failure Analysis, 2022, 132, 105931.	1.8	17
40	Prediction of Floor Failure Depth in Deep Coal Mines by Regression Analysis of the Multi-factor Influence Index. Mine Water and the Environment, 2021, 40, 497-509.	0.9	16
41	Dynamic Evolution and Identification of Bed Separation in Overburden During Coal Mining. Rock Mechanics and Rock Engineering, 2022, 55, 4015-4030.	2.6	16
42	Numerical simulation on crack propagation of rock mass with a single crack under seepage water pressure. Advances in Mechanical Engineering, 2017, 9, 168781401773289.	0.8	14
43	Ground stability evaluation of a coal-mining area: a case study of Yingshouyingzi mining area, China. Journal of Geophysics and Engineering, 2018, 15, 2252-2265.	0.7	14
44	Analysis of mining-induced variation of the water table and potential benefits for ecological vegetation: a case study of Jinjitan coal mine in Yushenfu mining area, China. Hydrogeology Journal, 2021, 29, 1629-1645.	0.9	14
45	Prediction of floor water disasters based on fractal analysis of geologic structure and vulnerability index method for deep coal mining in the Yanzhou mining area. Geomatics, Natural Hazards and Risk, 2019, 10, 1306-1326.	2.0	13
46	A new monitoring method for overlying strata failure height in Neogene laterite caused by underground coal mining. Engineering Failure Analysis, 2020, 117, 104796.	1.8	13
47	Hydrogeological Model for Groundwater Prediction in the Shennan Mining Area, China. Mine Water and the Environment, 2018, 37, 505-517.	0.9	11
48	Relevance Between Hydrochemical and Hydrodynamic Data in a Deep Karstified Limestone Aquifer: a Mining Area Case Study. Mine Water and the Environment, 2018, 37, 393-404.	0.9	11
49	Zoning for eco-geological environment before mining in Yushenfu mining area, northern Shaanxi, China. Environmental Monitoring and Assessment, 2018, 190, 619.	1.3	10
50	Coordinated exploitation of both coal and deep groundwater resources. Environmental Earth Sciences, 2020, 79, 1.	1.3	10
51	Study on the creep permeability of mining-cracked N2 laterite as the key aquifuge for preserving water resources in Northwestern China. International Journal of Coal Science and Technology, 2018, 5, 315-327.	2.7	8
52	An assessment of water yield properties for weathered bedrock zone in Northern Shaanxi Jurassic coalfield: a case study in Jinjitan coal mine, Western China. Arabian Journal of Geosciences, 2019, 12, 1.	0.6	8
53	Risk assessment of water inrushes from bed separations in Cretaceous strata corresponding to different excavation lengths during mining in the Ordos Basin. Geomatics, Natural Hazards and Risk, 2021, 12, 2300-2327.	2.0	8
54	Geological and geotechnical characteristics of N2 laterite in northwestern China. Quaternary International, 2019, 519, 263-273.	0.7	7

#	Article	IF	CITATIONS
55	Fuzzy comprehensive risk evaluation of roof water inrush based on catastrophe theory in the Jurassic coalfield of northwest China. Journal of Intelligent and Fuzzy Systems, 2019, 37, 2101-2111.	0.8	7
56	Evaluation of Groundwater Inflow into an Iron Mine Surrounded by an Imperfect Grout Curtain. Mine Water and the Environment, 2021, 40, 520-538.	0.9	7
57	Risk assessment of Cretaceous water inrush in the Ordos Basin based on the FAHP-EM. Water Policy, 2021, 23, 1249-1265.	0.7	7
58	Impact of mining-induced bed separation spaces on a cretaceous aquifer: a case study of the Yingpanhao coal mine, Ordos Basin, China. Hydrogeology Journal, 2022, 30, 691-706.	0.9	7
59	Geological Composition and Structure of the Filling Zone and Its Water-Resisting Property Evaluation on the Top of Ordovician Limestone. Geofluids, 2019, 2019, 1-15.	0.3	6
60	Vertical Shaft Excavation Shaping and Surrounding Rock Control Technology Under the Coupling Action of High Ground Stress and Fracture Formation. Journal of Performance of Constructed Facilities, 2020, 34, .	1.0	6
61	Beneficial Use of Deep Ordovician Limestone Water from Mine Safety Dewatering at the Xinglongzhuang Coal Mine, North China. Mine Water and the Environment, 2020, 39, 42-56.	0.9	4
62	Engineering geological and petrological characterization of paleoweathered rock in the K1/J2 contact zone in the Ordos Basin, China. Environmental Earth Sciences, 2022, 81, 1.	1.3	4
63	GIS-based evaluation of water-inrush risk from coal floor using logistic regression and certainty factor models. Arabian Journal of Geosciences, 2022, 15, 1.	0.6	3
64	Interaction mechanism of the interface between a deep buried sand and a paleo-weathered rock mass using a high normal stress direct shear apparatus. International Journal of Mining Science and Technology, 2015, 25, 623-628.	4.6	2
65	Experimental study on water–sand inrush characteristics and transport evolution in coal mines with N2 laterite. Arabian Journal of Geosciences, 2022, 15, 1.	0.6	1
66	Establishment and Application of Bed-Separation Water Inrush Coefficient Method Considering Water Resistance of Fractured Rock Mass. Geofluids, 2022, 2022, 1-19.	0.3	1
67	Height of overlying strata failure zone under different hydrogeological units. Environmental Earth Sciences, 2022, 81, 1.	1.3	1
68	Impacts of underground coal mining on phreatic water level variation in arid and semiarid mining areas: a case study from the Yushenfu mining area, China. Environmental Earth Sciences, 2022, 81, .	1.3	1
69	Method for Evaluating Fault Hydraulic Conductive Property and Its Application in Shandong, China. ACS Omega, 0, , .	1.6	1